A DESIGN ANALYSIS OF MICROMIRRORS IN STACKED CONFIGURATIONS WITH MOVING ELECTRODES

Sangtak Park, So-Ra Chung, and John T.W. Yeow
Department of Systems Design Engineering, University of Waterloo,
200 University Ave. W., Waterloo, Ontario, Canada
Email: jyeow@engmail.uwaterloo.ca

Abstract- Micromirrors fabricated by MEMS technology have demonstrated to be important sensing or actuating components in many industrial and biomedical applications such as laser scanning displays, optical switch matrices, and biomedical imaging systems. In this paper, various actuation mechanisms for micromirrors are described. A new geometric configuration of a stacked micromirror that is actuated by electrostatic force is proposed and analyzed to show its superior performance in terms of deflection angle, actuation voltage, and frequency response.

Index terms*:* Micromirror, MEMS, Electrostatic Force Actuation, Deflection Angle, Endoscope, OCT (Optical Coherence Tomography), Stacked Micromirror Configuration

I. INTRODUCTION

Development of MicroElectroMechanical Systems (MEMS) technology in the past decades has benefited automotive, communication and medical industries. Size and mass reduction that are enabled by MEMS technology have improved the performance of devices such as accelerometers, mass-flow sensors, bio-chips, RF devices, and automotive pressure sensors [1]. Popular MEMS devices for optical applications are optical switch arrays for communication [2], Optical Coherence Tomography (OCT) for an endoscope [3], confocal laser scanning microscopy (CLSM) for obtaining high resolution images, and digital micromirror devices for Digital Light Process (DLP) Projection.

MEMS micromirrors used for the above mentioned optical applications can be actuated via electrostatic, magnetic, thermal, and piezoelectric mechanisms. Various actuation mechanisms for sensing are presented in section II. Novel design and analytical modeling of electrostatic actuation of micromirror configuration are presented in section III. Geometry and design of stacked multiple electrode micromirror versus single micromirror configuration are

wide arm configuration with one end fixed to the substrate has nonlinear property due to temperature dependency [11].

2.4 Electrostatic Actuation:

Despite suffering from the pull-in effect, nonlinear behavior, and higher operating voltage, the electrostatic actuation's fast response time (less than 0.1 ms), low power consumption, and the easiness of integration and testing with electrical control system make the electrostatic actuation one of the preferred choices for micromirror actuation [12].

The operation voltage of the micromirror can be lowered while achieving more angular deflection if the stiffness of torsion bar is reduced. However, when the stiffness is lowered, the natural frequency of the micromirror also decreases, thereby reducing operational bandwidth. In this paper, two novel configurations of a stacked micromirror are presented. The proposed configuration has the potential to achieve more angular deflection at lower actuation voltage without sacrificing frequency response.

Table 1: Summary of Advantages and Disadvantages of Each Actuation Mechanism

Actuation	**Advantages**	**Disadvantages**
Magnetic	- Low actuation voltage - Relatively large angular deflection with lower driving power	- Difficult to assemble permanent magnets and coils with current CMOS technology - Challenge in minimizing the size of device
Piezoelectric	- Higher switching speed - Low power consumption	- Short actuation range
Thermal	- Ease of fabrication (require only one composite beam) for bulk production	- High power consumption - Slow response time - Fatigue due to thermal cycle
Electrostatic	- Low power consumption - Fast switching - Ease of integration and testing with electrical control circuitry	- Nonlinear characteristics - Limited by the pull-in effect - High actuation voltage - Fabrication complexity

I is the moment of the inertia of the micromirror.

c is the damping coefficient representing the squeeze-film damping.

k is the torsional stiffness of the rotated serpentine spring.

M is the torque created by the electrostatic force between the micromirror and its electrodes.

The moment of the inertia of the micromirror along the y axis is equal to $\frac{1}{12}ml^2$.

Second, the value for damping coefficient, **c**, representing the squeeze-film damping of the micromirror is derived from the linearized Reynold's equation [13] and presented in Equation (2).

$$C = -\frac{48\mu l w^3}{\pi^6 (b^2+4) D^3} \quad \ldots(2)$$

where,

μ is the dynamic viscosity of the air.

l is equal to the half length of the micromirror, $\frac{1}{2}L$.

w is the width of the micromirror.

b is the ratio of the width to the length of the micromirror.

D is the initial air gap between the micromirror and its electrodes.

$$M = \int_0^L x dF = \frac{\varepsilon w V^2}{2} \int_0^L \frac{x}{(D - x\sin\theta)^2} dx = \frac{\varepsilon w V^2}{2\sin^2\theta} \left\{ \frac{L\sin\theta}{D - L\sin\theta} + \ln\left(1 - \frac{L}{D}\sin\theta\right) \right\} \ldots(6)$$

where,

ε denotes the permittivity of air.

V represents the potential difference between the micromirror and its electrode.

Last, the normalized angle, φ, and the maximum deflection angle, θ_{max}, are defined as the following:

$$\varphi = \frac{\sin\theta}{\sin\theta_{max}} \approx \frac{\theta}{\theta_{max}},\ \theta_{max} = \sin^{-1}\frac{D}{L} \approx \frac{D}{L},\ if\ \theta \ll 1\ and\ \theta_{max} \ll 1 \ldots(7)$$

The torque, M, for each configuration is simplified with the normalized angle φ as represented by the following Equation (8) (9) and (10):

$$M_0 = \frac{1}{2}\varepsilon w V^2 \frac{L^2}{D^2}\frac{1}{\varphi^2}\left(\frac{\varphi}{1-\varphi} + \ln(1-\varphi)\right) \ldots(8)$$

$$M_1 = \frac{1}{2}\varepsilon w V^2 \frac{L^2}{D^2}\frac{1}{4\varphi^2}\left(\frac{2\varphi}{1-2\varphi} + \ln(1-2\varphi)\right) \ldots(9)$$

$$M_2 = \frac{1}{2}\varepsilon w V^2 \frac{L^2}{D^2}\frac{1}{2}\left(\frac{1}{1-2\varphi+\varphi^2}\right) \ldots(10)$$

IV. GEOMETRY

The size and geometry of the micromirror are determined by the diameter of the optical beam as well as its application. For example, a micromirror used in an endoscope would require a smaller form factor. In this paper, the micromirror is designed to be 1 mm in length, 1 mm in width and 10 μm in thickness. Also, it is assumed to be made of polysilicon that has a Young's modulus of 160 GPa, Poisson's ratio of 0.22 and density of 2330 kg/m^3. Normally, the micromirror is designed to be suspended over a cavity by two torsion bars. Even though a straight torsion bar is simple to design and fabricate, it suffers from residual stress, which alters the stiffness of a torsion bar and the micromirror's frequency response. Furthermore, modification of the physical or geometric properties of the straight torsion bar is not straightforward since the geometry of the torsion bar such as the width and thickness are limited by the fabrication process. Hence, two rotated serpentine springs are chosen to hold the micromirror in place while the micromirror rotates. The serpentine springs' stiffness can be easily customized regardless of the fabrication process. The rotated serpentine spring is well analyzed in [14] and has already been demonstrated [15]. Thus, a rotated serpentine spring is employed in this analysis. The rotated serpentine spring used in this analysis is 4 μm wide, 10 μm thick, and 100 μm in length from one end to another end. The gap between each turn is 4 μm. Figure 3(a) shows the expanded view of the rotated serpentine spring, and Figure 3(b) shows the relative size and location of the spring on the micromirror.

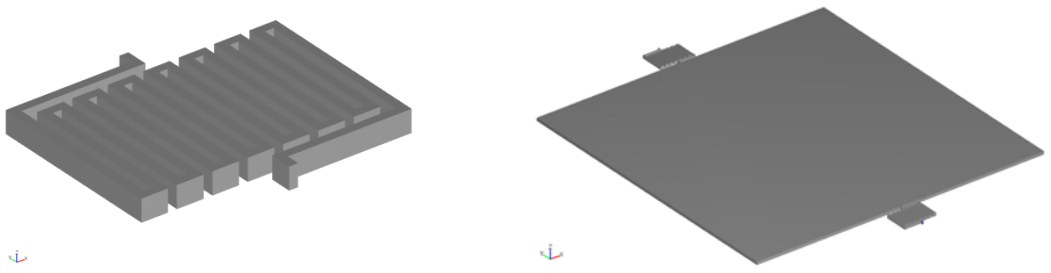

(a) (b)

Figure 3. (a) Rotated Serpentine Spring Torsion Bar and (b) the Micromirror.

V. NUMERIAL ANALYSIS AND RESUTLS

In this section, numerical analyses using COMSOL® are presented. The results are followed by a discussion on the static deflection that is caused by varying actuation voltages.

5.1 Finite Element Analysis (FEA):

The finite element models (FEM) are similar to the earlier analytical models other than the fact that the fixed bottom electrodes are located on the substrate. Three finite element models are created to represent each micromirror design configuration: (i) a single mirror with fixed bottom electrodes as shown in Figure 5(a); (ii) a stacked mirror on top of each other as shown in Figure 5(b); and (iii) a stacked mirror with an offset as shown in Figure 5(c). As mentioned before, the micromirror and its moving electrodes have the same size and material properties. Since all micromirrors are actuated by the electrostatic force, the air gap between the micromirror and its electrodes is also meshed with the arbitrary Lagrangian-Eulerian (ALE) method.

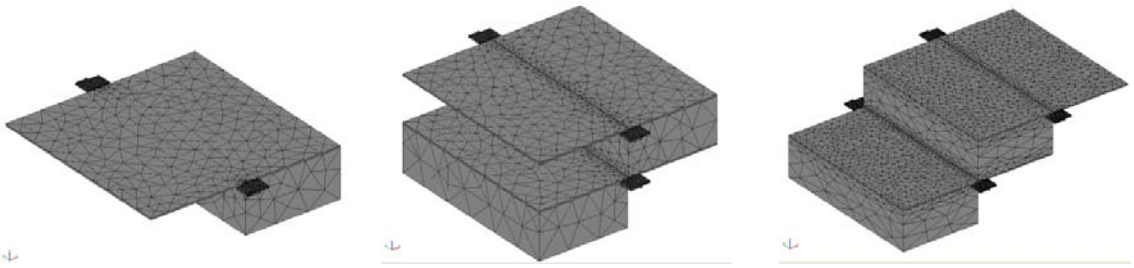

(a) (b) (c)

Figure 5. FEMs of the Three Micromirror Configurations.

5.2 Static Analysis:

In this static analysis, the DC voltage is increased gradually to find the deflection of the far edge of the moving plate (micromirror). The static analysis results of the three different configurations are shown in Figure 6. Both stacked mirrors show more deflection as the

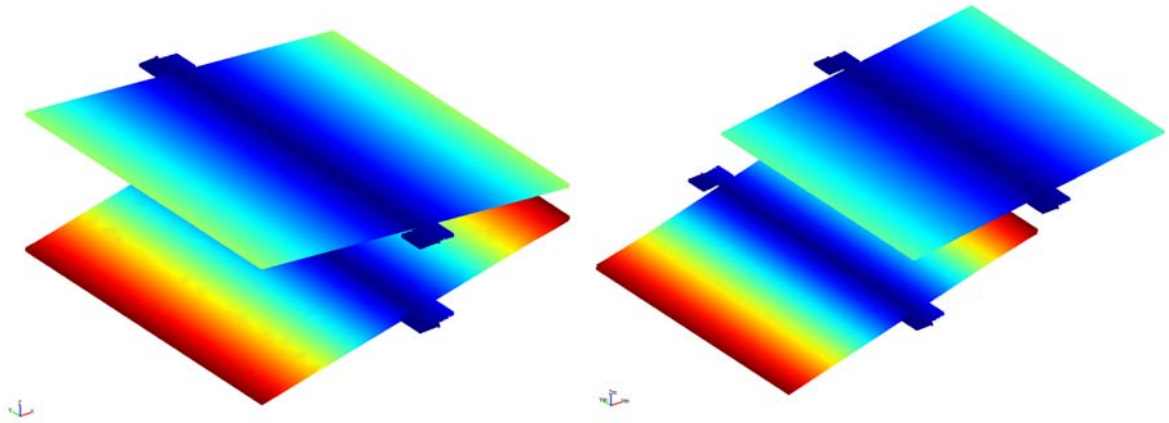

(a) (b)

Figure 7. Two Stacked Micromirror Configurations Post-Processed with the Deflection.

5.3 Normal Mode Analysis:

The normal mode analysis is performed to find the natural frequency of the micromirror using COMSOL®. Its first natural frequency is found to be 543 Hz when rotating about the Y- axis as shown in Figure 8(a). The second harmonic frequency is 3,602 Hz as a rectilinear motion along the Y axis (Figure 8(b)). The third harmonic frequency is 3,910 Hz as a rectilinear motion along the Z axis (Figure 8(c)). The fourth natural frequency is 5,268 Hz as a rectilinear motion along the X axis (Figure 8(d)). Note that the damping is not considered in this eigenfrequency analysis.

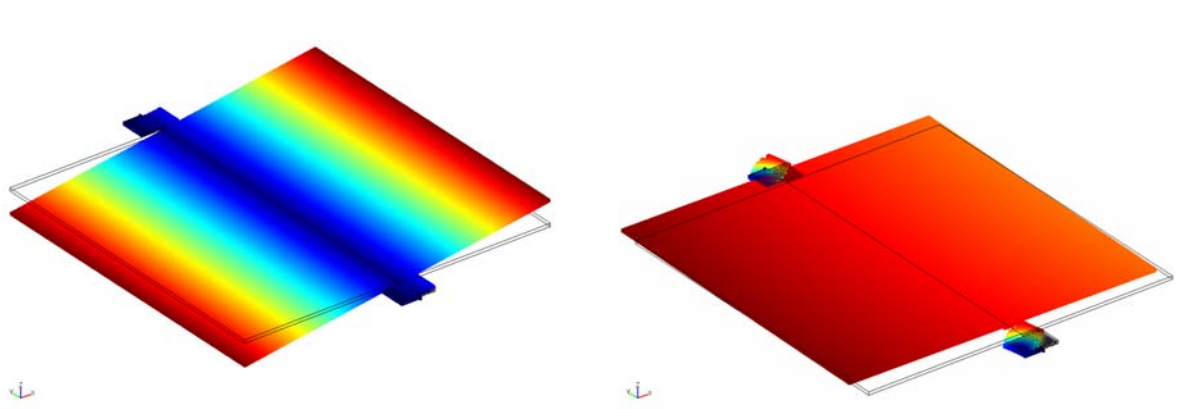

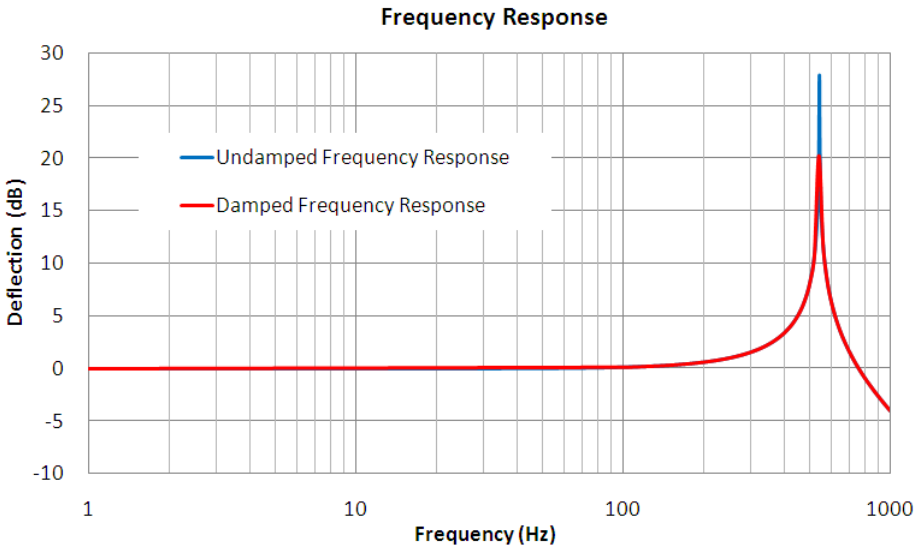

Figure 9. Frequency Response of the Micromirror.

5.5 Transient Analysis:

A 500Hz input AC voltage, with a fixed 80 Volts DC bias, is applied to find the transient performance of the micromirror. As mentioned before, most scanning micromirrors operate at their resonant mode to further increase its scanning angle. The control voltage signal is $80\sin(2\pi \cdot 500t) + 80$.

[2] Tze Wei Yeow, K. L. Eddie Law, and Andrew A. Goldenberg. "SOI-Based 2-D MEMS L-Switching Matrix for Optical Networking." *IEEE Jounal of Selected Topics in Quantum Electronics*, 2003: 603-613.

[3] J. T. W. Yeow, V. X. D. Yang, A. Chahwan, M. L. Gordon, B. Qi, I. A. Vitkin, B. C. Wilson, A. A. Goldenberg. "Micromachined 2-D scanner for 3-D optical coherence tomography." *Sensors and Actuators A:Physical*, 2005: 331-340.

[4] Takayuki Iseki, Miki Okumura and Takashi Sugawara. "Two-Dimensionally Deflecting Mirror Using Electromagnetic Actuation." *Optical Review*, 2006: 189-194.

[5] Orphee Cugat, Jerome Delamare, and Gilbert Reyne. "Magnetic Micro-Actuators and Systems (MAGMAS)." *IEEE Transactions on Magnetics*, 2003: 3607-3612.

[6] M R J Gibbs, E W Hill and P J Wright. "Magnetic materials for MEMS applications." *Journal of Physics D:Applied Physics*, 2004: R237-R244.

[7] Jonathan J. Bernstein, William P. Taylor, John D. Brazzle, Christopher J. Corcoran, Gregory Kirkos, Jefferson E. Odhner, Ajay Pareek, Marc Waelti, and Marvin Zai. "Electromagnetically Actuated Mirror Arrays for Use in 3-D Optical Switching Applications." *Journal of Microelectromechanical Systems*, 2004: 526-535.

[8] Robbins, William P. "High-Displacement Piezoelectric Actuator Utilizing a Meander-Line Geometry-Part II:Therory." *IEEETransactions on Ultrasonics, Ferroelectrics, and Frequency Control*, 1991: 461-467.

[9] Young Ho Seo, Doo-Sun Choi, Joon-Hyung Lee, Taik-Min Lee, Tae-Jin Je and Kyung-Hyun Whang. "Piezoelectric Actuator Based on Stiffness Control and Stroke Amplication for Large Lateral Actuation." *IEEE International Conference on Micro Electro Mechanical Systems*. 2005. 383-386.

[10] Janak Singh, Terence Gan, Ajay Agarwal, Mohanraj, Saxon Liw. "3D free space thermally actuated micromirror device." *Sensors and Actuators A: Physical*, 2005: 468-475.

[11] Atre, Amarendra. "Analysis of out-of-plane thermal microactuators." *Journal of Micromechanics and Microengineering*, 2006: 250-213.

[12] Jeffery F Rhoads, Steven W Shaw, and Kimberly L Turner, " The nonlinear response of resonant microbeam systems with purely-parametric electrostatic actuation" *Journal o f Micromechanics and Microengineering*, 2006: 890-899.

[13] Feixia Pan, Joel Kubby, Eric Peeters, Alex T. Tran, Subrata Mukherjee. "Squeeze Film Damping Effect on the Dynamic Response of a MEMS Torsion Mirror." *International Conference on Modeling and Simulation of Microsystems.* 1998. 474-479.